

Towards an Extended Microscopic Theory for the Upper fp-shell nuclei

K. P. Drumev, C. Bahri, and J. P. Draayer

Department of Physics and Astronomy, Louisiana State University, Baton Rouge, LA 70803, USA

V. G. Gueorguiev *

Lawrence Livermore National Laboratory, Livermore, CA 94551, USA

An extended SU(3) shell model that for the first time explicitly includes unique-parity levels is introduced. Shell-model calculations for the isotopes of ^{64}Ge and ^{68}Se are performed where valence nucleons beyond the $N=28=Z$ core occupy levels of the normal parity upper- fp shell ($f_{5/2}, p_{3/2}, p_{1/2}$) and the unique parity $g_{9/2}$ intruder configuration. The levels of the upper- fp shell are handled within the framework of an m-scheme basis as well as its pseudo-SU(3) counterpart, and respectively, the $g_{9/2}$ as a single level and as a member for the complete gds shell. It is demonstrated that the extended SU(3) approach allows one to better probe the effects of deformation and to account for many key properties of the system by using a highly truncated model space.

I. INTRODUCTION

The nuclear shell model [1] has been applied successfully for the description of various aspects of nuclear structure, in large part because it is based on a minimum number of assumptions. Although direct diagonalization of the Hamiltonian matrix in the full Hilbert space would be desirable, the dimensionality of such a space is often too large to allow calculations of this type to be done. Recently, in order to relax this restriction dramatically, various stochastic approaches, for instance, the Shell-Model Monte Carlo Method [2], have been suggested. Alternatively, algebraic models using the symmetry properties of the systems under investigation have been developed (e.g. [3, 4]).

Intruder levels are present in heavy deformed nuclei where the strong spin-orbit interaction destroys the underlying harmonic oscillator symmetry of the nuclear mean-field potential. The role they play for the overall dynamics of the system has been the topic of many questions and debates [5, 6, 7, 8]. Until now, the problem has been either approached within the framework of a truncation-free toy model [5] or by just considering the role of the single intruder level detached from its like-parity partners [6, 7]. It was argued in [5] that particles in these levels contribute in a complementary way to building the collectivity in nuclei. However, some mean-field theories suggest that these particles play the dominant role in inducing deformation [8]. In order to build a complete shell-model theory, these levels need to be included in the model space especially if experimentally observed high-spin or opposite-parity states are to be described.

Until recently, SU(3) shell-model calculations - real SU(3) [3] for light nuclei and pseudo-SU(3) [4] for heavy nuclei - have been performed in either only one space

(protons and neutrons filling the same shell, e.g. the ds shell) or two spaces (protons and neutrons filling different shells, e.g. for rare-earth and actinide nuclei). Various results for low-energy features, like energy spectra and electromagnetic transition strengths, have been published over the years [9, 10, 11]. These applications confirm that the SU(3) model works well for light nuclei and the pseudo-SU(3) scheme, under an appropriate set of assumptions, for rare-earth and actinide species. Up to now, SU(3)-based methodologies have not been applied to nuclei with mass numbers $A = 56$ to $A = 100$, which is an intermediate region where conventional wisdom suggests the break down of the assumptions that underpin their use in the other domains. In particular, the $g_{9/2}$ intruder level that penetrates down from the shell above due to the strong spin-orbit splitting appears to be as spectroscopically relevant to the overall dynamics as the normal-parity $f_{5/2}, p_{3/2}, p_{1/2}$ levels. Specifically, in this region the effect of the intruder level cannot be ignored or mimicked through a “renormalization” of the normal-parity dynamics which is how it has been handled to date.

The upper- $fp + g_{9/2}$ shell is the lightest region of nuclei where the intruder level must be taken into account. Its presence poses a significant challenge and opens a sequence of questions, many of them still unanswered. For example, if the pseudo-SU(3) symmetry proves to be a good scheme for characterizing upper- fp shell configurations, should one integrate the $g_{9/2}$ intruder into this picture by treating it as a single j -shell that is independent of couplings to the other members ($g_{7/2}, d_{5/2}, d_{3/2}, s_{1/2}$) of the gds shell, or should one take the complete gds shell into account? While the treatment of the $g_{9/2}$ intruder as a single additional orbit is possible for only a few exceptional nuclei within the m-scheme shell-model calculations, an SU(3) approach to the problem could allow the inclusion of the $g_{9/2}$ intruder as a member of the full gds shell and can be applied to all upper- fp nuclei. It is the purpose of this work to introduce and establish the benefits of a new and extended SU(3) shell model which, for the first time, explicitly includes particles from

*On leave of absence from Institute of Nuclear Research and Nuclear Energy, Bulgarian Academy of Sciences, Sofia 1784, Bulgaria.

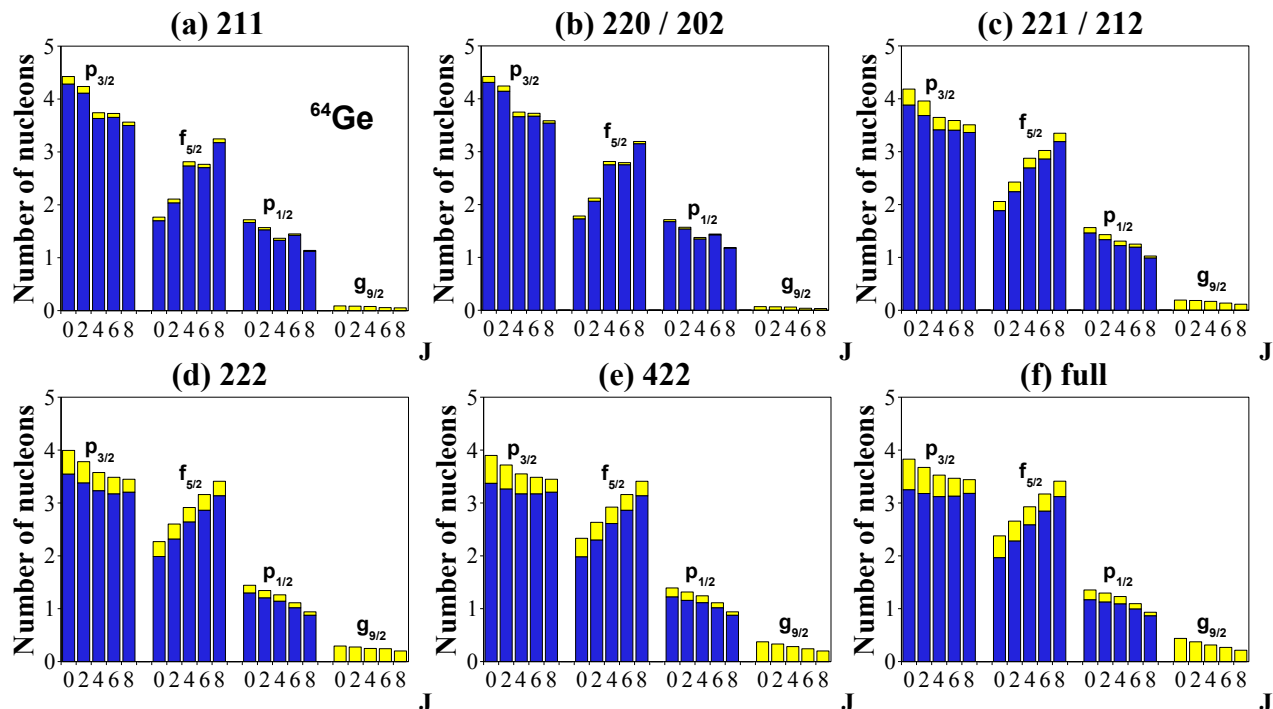


FIG. 1: (Color online) Single-particle occupation numbers for eigenstates of the g.s. band of ^{64}Ge calculated in different restricted model spaces (from (a) to (e)) and the full space (f). The labels TPN over each restricted-space calculation represent the maximum total number of particles T, and the maximum number of protons P (and neutrons N) allowed in the intruder $g_{9/2}$ level.

the complete unique-parity sector and therefore can be used to explore the role that intruder levels play in the dynamics of the system. Calculations are performed for two nuclei which are of major importance in astrophysics, namely, the waiting-point $N = Z$ nuclei ^{64}Ge and ^{68}Se [12]. In addition, ^{68}Se is known to be among the nuclei for which shape coexistence effects have been reported [13, 14]. Both the strengths and the limitations of the model are demonstrated and discussed.

First, a motivation for our approach is presented and the appropriate choice of model space is established by calculating, using a realistic Hamiltonian, the occupancies of the single-particle orbitals and the symmetry properties of these typical upper-fp shell nuclei. Then, following a brief introduction of the basics of the extended SU(3) model, calculations for the energy spectra, B(E2) transition strengths and the wave function content are performed and results are compared with the realistic predictions. Finally, discussion about various future applications of the model is included.

II. A REASONABLE APPROACH FOR THE DESCRIPTION OF UPPER FP-SHELL NUCLEI

To benchmark the benefit of the SU(3) scheme in this region (pseudo-SU(3) for the upper- fp shell and normal

SU(3) for the $g_{9/2}$ configurations extended to the full gds shell), we first generated results in a standard gds representation for both nuclei, ^{64}Ge and ^{68}Se , with the 8 (4 protons + 4 neutrons) and 12 (6 protons + 6 neutrons) valence nucleons, respectively, distributed across the $p_{1/2}, p_{3/2}, f_{5/2}, g_{9/2}$ model space with the $f_{7/2}$ level considered to be fully occupied and part of a ^{56}Ni core. The Hamiltonian we used is a G-matrix with a phenomenologically adjusted monopole part [15, 16] that in many cases describes the experimental energies reasonably well. Specifically, this upper- $fp + g_{9/2}$ shell interaction was successfully used in the past to obtain quite good results for nuclei like ^{62}Ga [17], and ^{76}Ge and ^{82}Se [15]. Later, it was applied for exploring the pseudo-SU(4) symmetry in the region from the beginning of the upper fp-shell up to $N = 30$ and for describing beta decays [18].

Calculations with different cuts of the full model space were done in order to estimate the occupancy of the single-particle levels and thus to evaluate the relative importance of various configurations for describing essential nuclear characteristics. In Fig. 1, a comparison is made between the occupancies for ^{64}Ge as determined in a restricted basis, where at most two particles (protons/neutrons) are allowed in the $g_{9/2}$ level and the full-space results. The upper (yellow) bars show the contri-

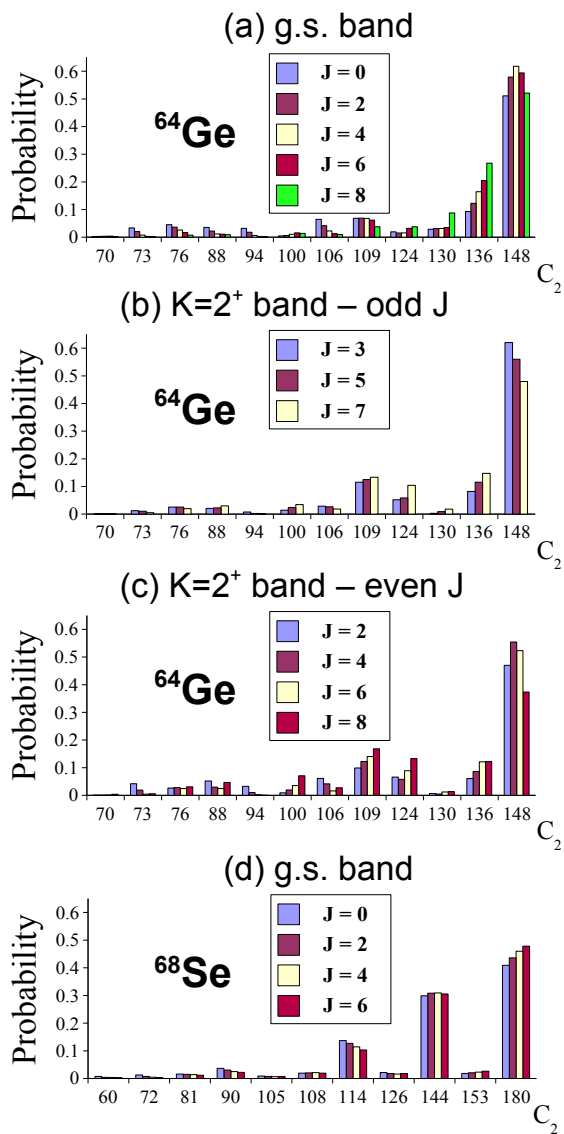


FIG. 2: (Color online) Pseudo-SU(3) content of the low-lying states in (a) the g.s. band of ^{64}Ge , (b) and (c) - the $K = 2^+$ band of ^{64}Ge , and (d) the g.s. band of ^{68}Se using the renormalized counterpart of the G-matrix realistic interaction.

tribution to occupations from basis states with an occupied intruder level while the lower (blue) portion represents those where the intruder level is empty. The calculated results suggest that the occupancy probability for the intruder level is approximately 0.3 particles for the low-lying states of ^{64}Ge . Calculations with no particles allowed in the intruder level or with just one identical-particle (or proton-neutron) pair (Fig. 1 (a) and (b)) cannot describe either its occupancy or the gradual change in the occupancy of the single-particle levels in the ground-state (g.s.) band that is found in the full-model-space results. However, using a restricted space with at most two identical particles occupying the intruder level (in Fig. 1(e)) is sufficient to describe both features as

well as the low-energy spectrum and the B(E2) transition strengths [19]. Similar results were observed for the $K = 2^+$ band of this nucleus. As expected, calculations for ^{68}Se performed in a truncated basis with at most 2 nucleons allowed in the intruder level produce a slightly higher value of the $g_{9/2}$ occupancy compared to ^{64}Ge .

Next, the goodness of the pseudo-SU(3) symmetry in these nuclei was tested using a renormalized version of the same realistic interaction in the $pf_{5/2}$ space [18]. The matrix of the second-order Casimir operator of pseudo-SU(3), $C_2 = \frac{1}{4}(3\hat{L}^2 + Q \cdot Q)$, was generated and the method of moments [20] used to diagonalize this matrix by starting the Lanczos procedure with specific eigenvectors of the Hamiltonian for which a pseudo-SU(3) decomposition was desired. Although the procedure provides distributions only over the C_2 values (and not over the actual (λ, μ) irreducible representations (irreps)) this analysis is quite useful and gives valuable information about the structure of certain eigenstates.

The distribution of the second order Casimir operator C_2 of pseudo-SU(3) yields contributions of about 50-60% from the leading pseudo-SU(3) irrep in the g.s. band of ^{64}Ge (Fig. 2(a)) which suggests that the pseudo-SU(3) symmetry is quite good. In the $K = 2^+$ band (Fig. 2 (b) and (c)) this contribution appears to be somewhat lower, ranging from approximately 37% for the 8_2^+ state to about 62% in the 3_1^+ state. The analysis also reveals that using only five irreps which have the highest C_2 value one may take account of at least 70% and up to about 95% of the wavefunction for the states in these bands.

In the case of ^{68}Se , the outcome turns out to be quite similar for the states from the g.s. band (Fig. 2(d)). Although the irreps with the maximal value of $C_2 = 180$ participate with only between about 40% and 50%, the first eleven irreps with distinct values of λ and μ account for 88-93% of the wavefunction. In addition, the 0_3^+ state at 2.51 MeV is also dominated (64%) by irreps with the biggest C_2 value. However, other states are predicted to be highly-mixed SU(3) configurations. This includes the 0_2^+ state found at 1.05 MeV - a value very similar to the ones reported in [13, 14] for a low-lying state of prolate shape. A recent analysis reveals that many low-lying states in other $N \sim Z$ nuclei also have good pseudo-SU(3) symmetry which further underscores the value of using symmetry-based truncation schemes [19].

In summary, the outcome of the m-scheme study has demonstrated that only part of the configurations are relevant for the structure of the low-lying states in the upper-fp shell nuclei. This along with the pseudo-SU(3) spectral decomposition of the states establishes the validity of a SU(3)-based truncation scheme in $N \sim Z$ upper-fp shell nuclei. As for the unique-parity spaces, the so-called quasi-SU(3) concept [9, 10, 21] may also be applicable, however, this question is deferred to a follow-on investigation. Since (as we will see below) the role of the unique-parity spaces for the nuclei we deal with, is to introduce only some high-order effects, it is relatively safe to accept this to be true throughout the current work.

III. AN EXTENDED SU(3) MODEL WITH EXPLICITLY INCLUDED INTRUDER LEVELS

Following the series of arguments and motivations presented in the previous section, we can now introduce the basics of the extended SU(3) shell model. Like its early precursors [3, 4], it is also a microscopic theory in the sense that both SU(3) generators - the angular momentum ($L_\mu, \mu = 0, \pm 1$) and quadrupole ($Q_\mu; \mu = 0, \pm 1, \pm 2$) operators - are given in terms of individual nucleon coordinate and momentum variables. However, the model space has a more complicated structure than the one used in earlier models based on the SU(3) symmetry. Specifically, it consists of two parts for each particle type, a normal (N) parity pseudo-shell ($f_{5/2}, p_{3/2}, p_{1/2} \rightarrow \tilde{d}_{5/2}, \tilde{d}_{3/2}, \tilde{s}_{1/2}$) and a unique (or abnormal) (U) parity shell composed of all levels of opposite parity from the *gds* shell above. (Since the normal-unique space distinction will be obvious from context, we will not place tildes over pseudo-space labels as is normally done.)

The many-particle basis states

$$\{|a_\pi; a_\nu\rangle \rho(\lambda, \mu) \kappa L, \{S_\pi, S_\nu\} S; JM\} \quad (1)$$

are built as SU(3) proton (π) and neutron (ν) coupled configurations with well-defined particle number and good total angular momentum. Here, the proton and neutron quantum numbers are indicated by $a_\sigma = \{a_{\sigma N}, a_{\sigma U}\} \rho_\sigma(\lambda_\sigma, \mu_\sigma)$, where the $a_{\sigma\tau} = N_{\sigma\tau} [f_{\sigma\tau}] \alpha_{\sigma\tau}(\lambda_{\sigma\tau}, \mu_{\sigma\tau})$ are the basis-state labels for the four spaces in the model (σ stands for π or ν , and τ stands for N or U). In the last expression, $N_{\sigma\tau}$ denotes the number of particles in the corresponding space, $[f_{\sigma\tau}]$ - the spatial symmetry label and $(\lambda_{\sigma\tau}, \mu_{\sigma\tau})$ - the SU(3) irrep label. Multiplicity indices $\alpha_{\sigma\tau}$ and ρ_σ count different occurrences of $(\lambda_{\sigma\tau}, \mu_{\sigma\tau})$ in $[f_{\sigma\tau}]$ and in the product $\{(\lambda_{\sigma N}, \mu_{\sigma N}) \times (\lambda_{\sigma U}, \mu_{\sigma U})\} \rightarrow (\lambda_\sigma, \mu_\sigma)$, respectively. First, the particles from the normal and the unique spaces are coupled for both protons and neutrons. Then, the resulting proton and neutron irreps are coupled to a total final set of irreps. The total angular momentum J results from the coupling of the total orbital angular momentum L with the total spin S . The ρ and κ are, respectively, the multiplicity indices for the different occurrences of (λ, μ) in $\{(\lambda_\pi, \mu_\pi) \times (\lambda_\nu, \mu_\nu)\}$ and L in (λ, μ) .

The Hamiltonian

$$H = \sum_{\sigma, \tau} (H_{sp}^{\sigma\tau} - GS^{\sigma\tau\dagger} S^{\sigma\tau}) - \frac{\chi}{2} : Q \cdot Q : + aJ^2 + bK_J^2 - G \left(\sum_{\sigma, \tau \neq \tau'} S^{\sigma\tau\dagger} S^{\sigma\tau'} + \sum_{\tau, \tau'} S^{\pi\nu, \tau\dagger} S^{\pi\nu, \tau'} \right) \quad (2)$$

includes spherical Nilsson single-particle energies

$$H_{sp}^{\sigma\tau} = \sum_{i_{\sigma\tau}} (H_0 + C_{\sigma\tau} \mathbf{l}_{i_{\sigma\tau}} \cdot \mathbf{s}_{i_{\sigma\tau}} + D_{\sigma\tau} l_{i_{\sigma\tau}}^2) \quad (3)$$

as well as the quadrupole-quadrupole and pairing interactions (within a shell and between shells) plus two rotor-like terms that are diagonal in the SU(3) basis. In general, the harmonic oscillator term, $H_0 = \hbar\omega(\eta_{i_{\sigma\tau}} + \frac{3}{2})$

where $\hbar\omega \approx \frac{41}{A^{1/3}}$ [22], is essential and its contribution does not cancel out when more than one possible distribution of particles over the shells is involved. The colons in the quadrupole operator notation represent normal-ordered operator since all the one-body effects have already been taken into account by the single-particle terms in the Hamiltonian. In addition, in first approximation, the quadrupole operator in the normal-parity spaces is related to its pseudo counterpart by $Q_{\sigma N} \approx \frac{\tilde{\eta}+1}{\tilde{\eta}} \tilde{Q}_{\sigma N}$ with $\tilde{\eta}$ equal to 2 for both protons and neutrons and $Q = Q_{\pi N} + Q_{\pi U} + Q_{\nu N} + Q_{\nu U} \approx 1.5 \tilde{Q}_{\pi N} + Q_{\pi U} + 1.5 \tilde{Q}_{\nu N} + Q_{\nu U}$.

TABLE I: Parameters (in MeV) used in the extended SU(3) model Hamiltonian.

Nucleus	G	χ	a	b
^{64}Ge	0.280	0.0176	-0.002	0.020
^{68}Se	0.263	0.0152	-0.002	0.000

The second line in Eq.(2) consists of pairing terms that are included for the first time in SU(3) shell-model calculations. In particular, the first term represents the scattering of an identical-particle pair between the normal- and unique-parity spaces. The second one stands for the proton-neutron pairing (or simply pn-pairing) interaction within the normal- or unique-parity space (terms with $\tau = \tau'$) and for the pn-pair scattering between the normal- and unique-parity spaces (terms with $\tau \neq \tau'$). The formulae used in this work for each type of pairing operator can be found in the Appendix A. It is worth mentioning that, contrary to many calculations involving the pairing interaction, these expressions are exact. Finally, the two rotor-like terms J^2 and K_J^2 (the square of the total angular momentum and its projection on the intrinsic body-fixed axis) are used to “fine tune” the energy spectra, adjusting the moment of inertia of the g.s. band and the position of the $K = 2^+$ bandhead, respectively. Their strengths are the only two parameters fitted in this work.

The single-particle terms together with the proton, neutron and proton-neutron pairing interactions mix the SU(3) basis states, which allows for a realistic description of the energy spectra of the nuclei. The values of the parameters used in Hamiltonian (2) can be found in Table I. The single-particle energies in the Hamiltonian for the normal spaces are fixed with the numbers provided by the upper-fp shell single-particle energies and for the strengths in the unique-parity spaces the numbers from systematics are used [22]. The values for the parameters G and χ in the Hamiltonian which are taken from [23] are found to be in agreement with the ones [22, 24] used in previous calculations for some ds-shell and rare-earth nuclei. For simplicity, we take both identical-particle and proton-neutron pairing strengths to be equal.

TABLE II: The irreps in the coupled proton-neutron model space for ^{64}Ge and ^{68}Se that were used in the extended SU(3) shell-model calculations. The subscripts for each spin value denote the multiplicity, that is, the number of different ways the corresponding irrep can be constructed.

$[N_{\pi N}, N_{\pi U}; N_{\nu N}, N_{\nu U}]$		total $(\lambda, \mu)S_{\text{multiplicity}}$			
^{64}Ge					
[4, 0; 4, 0]	(8, 4)0 ₁	(9, 2)0 _{1, 12}	(10, 0)0 _{2, 11, 21}	(6, 5)0 _{1, 12}	(7, 3)0 _{6, 18, 22}
[4, 0; 2, 2] [2, 2; 4, 0]	(16, 2)0 ₂	(17, 0)1 ₂	(14, 3)0 _{6, 16}	(15, 1)0 _{12, 115, 24}	(12, 4)0 _{18, 118, 24}
[3, 1; 3, 1]	(16, 2)0 _{2, 13, 21}	(17, 0)0 _{2, 13, 21}	(14, 3)0 _{8, 115, 25}	(15, 1)0 _{16, 127, 210}	(12, 4)0 _{28, 143, 215}
[2, 2; 2, 2]	(24, 0)0 ₁	(22, 1)0 _{3, 14}	(20, 2)0 _{16, 118, 24}	(21, 0)0 _{9, 118, 24}	(18, 3)0 _{42, 164, 216}
^{68}Se					
[6, 0; 6, 0]	(12, 0)0 ₁ (1, 10)0 _{1, 12} (2, 8)0 _{8, 112, 24}	(0, 12)0 ₁ (6, 6)0 _{4, 13, 21}	(9, 3)0 _{2, 12} (7, 4)0 _{6, 111, 23}	(3, 9)0 _{2, 12} (4, 7)0 _{6, 111, 23}	(10, 1)0 _{1, 12} (8, 2)0 _{8, 112, 24}
[6, 0; 4, 2] [4, 2; 6, 0]	(18, 2)0 ₂ (17, 1)0 _{12, 116, 24}	(19, 0), 1 ₂ (13, 6)0 _{10, 116, 24}	(15, 5)0 _{2, 12}	(16, 3)0 _{8, 112, 22}	(12, 8)0 ₂
[5, 1; 5, 1]	(18, 2)0 _{2, 13, 21} (17, 1)0 _{18, 130, 214}	(19, 0)0 _{2, 13, 21} (13, 6)0 _{20, 133, 215}	(15, 5)0 _{4, 16, 22}	(16, 3)0 _{16, 127, 213}	(12, 8)0 _{2, 13, 21}
[4, 2; 4, 2]	(24, 4)0 ₁ (24, 1)0 _{19, 131, 213}	(25, 2)0 _{1, 12} (20, 6)0 _{16, 118, 26}	(26, 0)0 _{2, 11, 21}	(22, 5)0 _{3, 14}	(23, 3)0 _{14, 120, 26}

IV. RESULTS AND DISCUSSION

Calculations within the framework of the extended SU(3) model were performed using irreps from 5 types of configurations - for example, $[N_{\pi N}, N_{\pi U}; N_{\nu N}, N_{\nu U}] = [4, 0; 4, 0]$, $[4, 0; 2, 2]$, $[2, 2; 4, 0]$, $[3, 1; 3, 1]$ and $[2, 2; 2, 2]$ for the ^{64}Ge case. (See Table II where the list of configurations for ^{68}Se is also given.) For each of these groups, irreps in the proton and neutron spaces with (pseudo-) spin $S_{\sigma\tau} = 0, 1/2, 1$ and $3/2$ in both the normal- and the unique-parity spaces were generated. Then, from all the possible couplings between these we chose those with the largest value of the second order Casimir operator of SU(3) and spin $S = 0, 1$ and 2 . Here, we present results obtained with five (seven) coupled proton-neutron irreps with distinct values of λ and μ for each distribution of particles between the normal and unique spaces for ^{64}Ge (^{68}Se). (This number was even pushed up to eleven for the $[6, 0; 6, 0]$ configuration in ^{68}Se). The complete set, listed in Table II, consists of 492 (580) coupled irreps in the case of ^{64}Ge (^{68}Se). This number is bigger by a factor of about 20 than the one typically handled up to now within the framework of the SU(3) model. Some of the coupled irreps can be constructed in more than one way.

For example, the irrep $(\lambda, \mu)S = (10, 0)0$ can be obtained by coupling the $(\lambda_{\pi}, \mu_{\pi})S_{\pi} \times (\lambda_{\nu}, \mu_{\nu})S_{\nu} = (4, 2)0 \times (4, 2)0$ or $(5, 0)1 \times (5, 0)1$ proton and neutron irreps.

For both ^{64}Ge and ^{68}Se , proton-neutron configurations with no particles in the unique space are found, as expected, to lie lowest and determine, by-and-large, the structure of the low-lying eigenstates. Only a small portion of all proton-neutron coupled irreps - 27 (112) in the case of ^{64}Ge (^{68}Se) - belong to these types of configurations, which we will refer to as the dominant ones. Since the only possible irrep in the unique-parity spaces for this case is $(\lambda_{\pi U}, \mu_{\pi U}) = (0, 0)$ (and $(\lambda_{\nu U}, \mu_{\nu U}) = (0, 0)$), these configurations are the exact pseudo analog of the ones encountered in the ds-shell nuclei ^{24}Mg and ^{28}Si which have been studied earlier [9]. Using only the principal part of the Hamiltonian (2), namely, the part with both rotor term strengths equal to zero, we are able to provide a good description of the low-lying states. Specifically, all the energies from the g.s. bands (with the exception of the 2_1^+ state in ^{68}Se) differ by no more than 15% from the experimental values [25]. In order to conform with this result and prevent any further changes in the structure of the wave function, the range of values for the parameters a and b were severely restricted so that these terms only introduce small ("fine tuning") changes

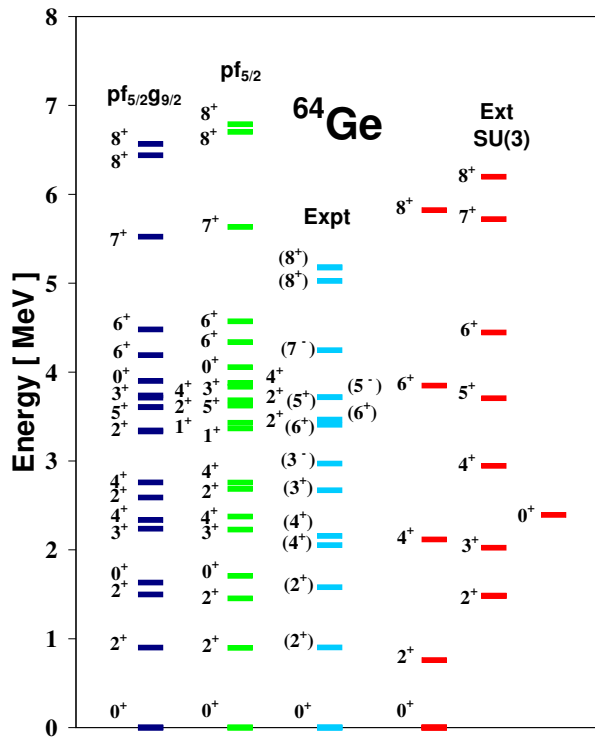


FIG. 3: (Color online) Low-energy spectra of ^{64}Ge obtained with (from left to right) the realistic interaction in the full $pf_{5/2}g_{9/2}$ and $pf_{5/2}$ model spaces compared with experiment [25] and the extended-SU(3)-model results.

to the overall fit.

Proton-neutron configurations with two and four particles in the unique-parity space prevail at higher energies. The former starts to dominate from about 3.5 MeV (5 MeV) in the case of ^{64}Ge (^{68}Se), usually for states of higher spin values, and the latter at even higher energies. The amount of mixing found between configurations with different distribution of particles is due to the pair-scattering interactions between the normal- and unique-parity spaces. While the expected behavior of the unique-parity-space occupancy is observed - it goes up with the rise of both G and/or χ strengths - with the choice of parameters from Table I the absolute values appear to be underestimated by at least a factor of 3 in ^{64}Ge (see the result shown in Fig. 1) and by even more for the case of ^{68}Se . This may indicate that the model space has to be further expanded to accommodate more mixing from the pair-scattering interaction terms, that the pn-interaction indeed should enter with different, possibly bigger strength than the identical-particle pairing, or the possible need to include other terms in the Hamiltonian like the quadrupole and isoscalar pairing interactions.

Results for the excitation spectra of ^{64}Ge are presented in Fig. 3. The realistic G-matrix interaction gives a reasonable result for the low-lying states consistent with the one obtained in [13, 23]. Moreover, a description

of a similar quality is provided by the extended SU(3) model. The existence of two prolate bands, as predicted by the calculations with the realistic interactions, is also observed, that is, a g.s. $K = 0^+$ and an excited $K = 2^+$ band, both dominated by the (8, 4) irrep. The first excited 0^+ (0_2^+) state, not reported yet experimentally, is found at 2.39 MeV which is higher than the prediction made by the realistic interactions.

Consistent with the outcome for ^{64}Ge , in the case of ^{68}Se we found a reasonable description for the energies of the states from the g.s. band (Fig. 4). Even the use of a restricted space with at most 2 nucleons allowed in the intruder $g_{9/2}$ level produces result which reflects some basic characteristics of the full-space spectrum reported in [13]. For example, the first excited 0^+ state (0_2^+) is also positioned below the 2_2^+ state. A new feature observed in our results is that the 0_3^+ state at 2.51 MeV was found to be dominated by the shapes with $C_2 = 180$ (see Section II). Within the framework of the extended SU(3) shell model, ^{68}Se is predicted to be a mid-shell nucleus, a fact which may explain the existence of shape coexistence effects. Unlike the case of ^{28}Si [9], now the g.s. band is dominated by the irrep (12, 0) which corresponds to a prolate shape. This result mainly follows due to the presence of

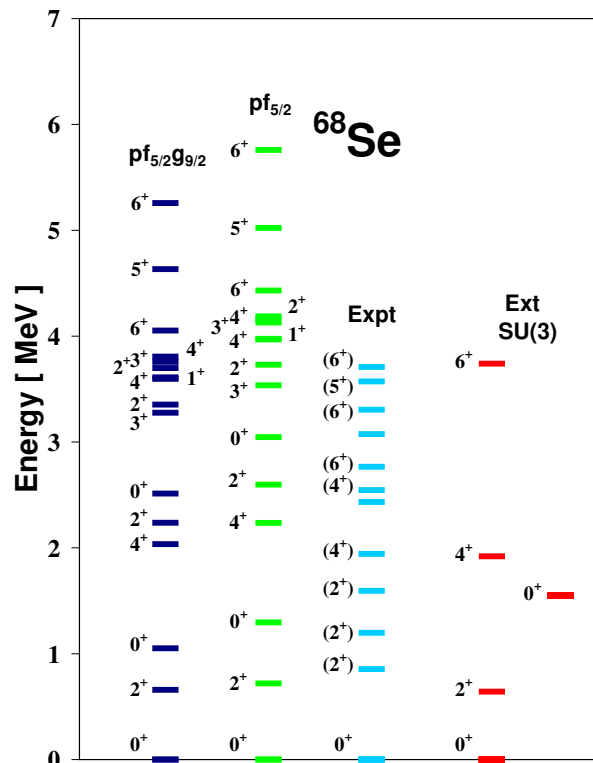


FIG. 4: (Color online) Low-energy spectra of ^{68}Se obtained with (from left to right) the realistic interaction in the restricted $pf_{5/2}g_{9/2}$ (at most 2 particles allowed in the intruder $g_{9/2}$ level) and full $pf_{5/2}$ model spaces compared with experiment [25] and the extended-SU(3)-model results.

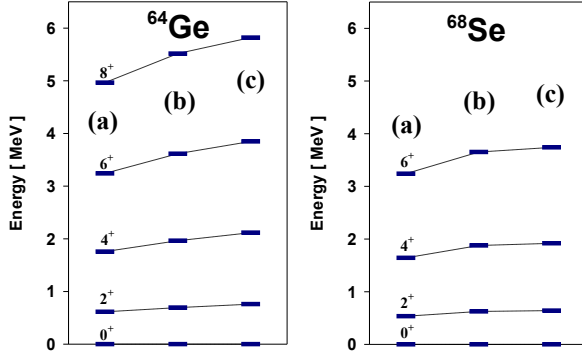


FIG. 5: (Color online) Role of the pn-pairing and the pair-scattering terms for the states in the g.s. band of ^{64}Ge and ^{68}Se : (a) both pair-scattering and pn-pairing contributions excluded, (b) only pair-scattering contribution excluded and (c) total interaction.

the orbit-orbit terms in the Hamiltonian and is in agreement with some earlier discussions [26, 27]. Specifically, it favors the scenario in which the lower eigenstates in the g.s. band are prolate and throughout the band the shape changes to oblate [26]. Because of the nature of the leading representation, the model can not easily account for a $K = 2^+$ band with the same shape characteristic, neither can it give a simple explanation for a low-lying $K = 0^+$ band, facts which are in support of the realistic prediction made in Section II for a highly-mixed nature of the 0_2^+ as well as many other low-lying states in this nucleus. With only the J^2 term used in the Hamiltonian for adjusting the energies, the 0_2^+ state is predicted by the model at 1.55 MeV.

The effect of adding the proton-neutron pairing and the pair-scattering terms in the Hamiltonian is illustrated in Fig. 5. For our choice of model space (Table II), the results for the g.s. bands demonstrate comparable size effects from both interactions, especially for ^{64}Ge , with the only clear exception being the 4_1^+ and 6_1^+ states in ^{68}Se . When a smaller number of irreps is included in the calculation, the pn-pairing interaction has a much bigger impact, an effect mainly visible for higher-spin states, while the role of the pair-scattering terms is strongly diminished.

Electromagnetic transition strengths are normally calculated with the E2 transition operator of the form [7, 28]:

$$T(E2) \approx \sqrt{5/16\pi} A^{1/3} (e_\pi \frac{\tilde{\eta}_\pi + 1}{\eta_\pi} \tilde{Q}_{\pi N} + e_\pi Q_{\pi U} + e_\nu \frac{\tilde{\eta}_\nu + 1}{\eta_\nu} \tilde{Q}_{\nu N} + e_\nu Q_{\nu U}) \quad (4)$$

Instead, in this work we simply used the single dominant component in the pseudo-SU(3) expansion of the quadrupole operators in the normal-parity space. The effective charges e_π and e_ν were taken as $e_\pi = 1.5$ and $e_\nu = 0.5$ for the two versions of the realistic interac-

TABLE III: $B(E2)$ transition strengths for ^{64}Ge in units of $e^2 fm^4$ calculated using the G-matrix interaction in full $pf_{5/2}$ and $pf_{5/2}g_{9/2}$ model spaces, and the extended SU(3) model. Entries in parentheses show the result when only the normal spaces are used in the calculations.

$(J+2)^+ \rightarrow J^+$	$pf_{5/2}$	$pf_{5/2}g_{9/2}$	Ext. SU(3)
$2_{g.s.}^+ \rightarrow 0_{g.s.}^+$	257.22	253.91	292.80 (280.10)
$4_{g.s.}^+ \rightarrow 2_{g.s.}^+$	332.54	342.51	346.26 (334.10)
$6_{g.s.}^+ \rightarrow 4_{g.s.}^+$	340.51	356.92	380.39 (370.56)
$8_{g.s.}^+ \rightarrow 6_{g.s.}^+$	303.31	320.14	273.84 (268.08)
<hr/>			
$4_\gamma^+ \rightarrow 2_\gamma^+$	89.26	93.13	67.25 (65.73)
$6_\gamma^+ \rightarrow 4_\gamma^+$	164.23	144.19	207.18 (204.78)
$8_\gamma^+ \rightarrow 6_\gamma^+$	92.12	84.38	74.79 (79.39)
<hr/>			
$(J+1)^+ \rightarrow J^+$			
$3_\gamma^+ \rightarrow 2_\gamma^+$	371.15	357.79	505.27 (493.39)
$5_\gamma^+ \rightarrow 4_\gamma^+$	238.48	240.40	137.48 (135.48)
$7_\gamma^+ \rightarrow 6_\gamma^+$	159.44	161.24	10.26 (10.17)
<hr/>			
$J_\alpha^+ \rightarrow J_\beta^+$			
$2_\gamma^+ \rightarrow 0_{g.s.}^+$	1.98	1.42	5.71 (5.74)
$2_\gamma^+ \rightarrow 2_{g.s.}^+$	251.68	241.41	183.16 (178.96)
$3_\gamma^+ \rightarrow 2_{g.s.}^+$	4.21	3.40	9.90 (9.93)
$4_\gamma^+ \rightarrow 4_{g.s.}^+$	72.10	74.69	47.11 (46.89)
$4_\gamma^+ \rightarrow 2_{g.s.}^+$	18.86	19.31	6.70 (6.75)

TABLE IV: $B(E2)$ transition strengths for the states in the g.s. band of ^{68}Se in units of $e^2 fm^4$ calculated using the G-matrix interaction in full $pf_{5/2}$ model space and the extended SU(3) model. Entries in parentheses show the result when only the normal spaces are used in the calculations.

$(J+2)^+ \rightarrow J^+$	$pf_{5/2}$	Ext. SU(3)
$2_{g.s.}^+ \rightarrow 0_{g.s.}^+$	322.71	354.17 (346.37)
$4_{g.s.}^+ \rightarrow 2_{g.s.}^+$	448.07	486.65 (477.18)
$6_{g.s.}^+ \rightarrow 4_{g.s.}^+$	441.58	473.89 (467.09)

tion and the extended-SU(3) calculations. The overall agreement between the results for both nuclei (Table III for ^{64}Ge and Table IV for the g.s. band in ^{68}Se) is good, although some recent experimental findings for the $2_{g.s.}^+ \rightarrow 0_{g.s.}^+$ transition strength in ^{64}Ge [29] seem to be underestimated by approximately a factor of 1.4. The correct behavior of the interband transitions is also nicely reproduced. More significant deviations are observed for the transitions between members of the $K = 2^+$ band and the $(J+1)^+ \rightarrow J^+$ transitions in ^{64}Ge . These could be attributed to the fact that some of the states from this band (e.g. 4_2^+ and 6_2^+) are found to be highly mixed with $S = 1$ irreps and differ more significantly from the rest thus displaying a less regular structure pattern throughout the band, for example, to what has been observed in the same bands of some rare-earth nuclei. It seems that the orbit-orbit interaction is the part of the

TABLE V: Model-space dimensions for the G-matrix calculations in the full (restricted) $pf_{5/2}g_{9/2}$ space for ^{64}Ge (^{68}Se) as well as for the complete $pf_{5/2}$ spaces and for the extended SU(3) shell model with the irreps listed in Table II. (The entry marked with a * is smaller by about a factor of two due to our taking advantage of time-reversal symmetry, which we did not invoke in the other cases as machine storage for them was not an issue.)

	J				
	0	2	4	6	8
	^{64}Ge				
$pf_{5/2}g_{9/2}$	1,831,531	1,728,929	1,454,930	1,090,581	724,318
$pf_{5/2}$	28,503	24,246	14,760	6,183	1,638
Ext. SU(3)	322	1,421	2,098	2,225	2,208
	^{68}Se				
$pf_{5/2}g_{9/2}$	1,929,014*	3,611,680	2,973,404	2,138,391	
$pf_{5/2}$	93,710	81,122	52,175	37,086	
Ext. SU(3)	397	1,765	2,640	3,115	

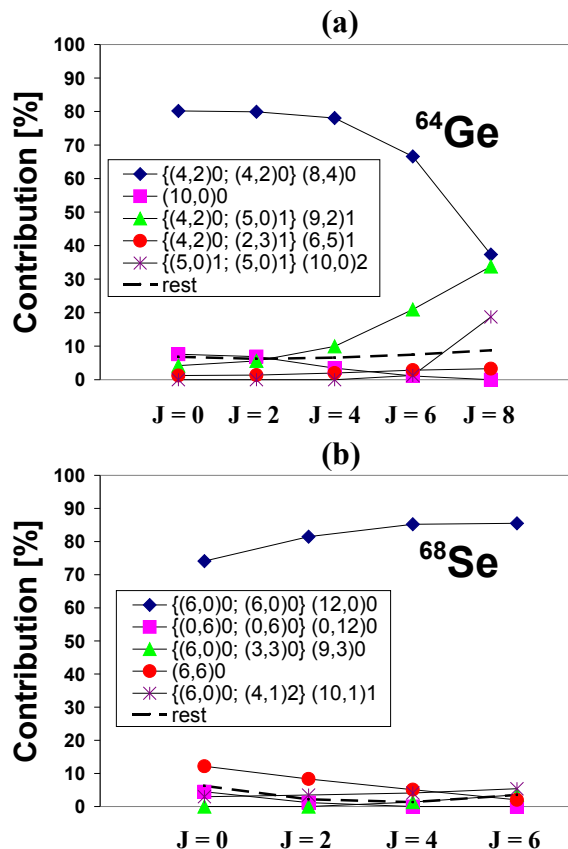


FIG. 6: (Color online) Wave-function decomposition of the calculated extended SU(3) eigenstates in the g.s. band of (a) ^{64}Ge and (b) ^{68}Se . The leading irreps from the dominant type configurations are listed explicitly while the effect of those with less than 3% contribution for any state as well as from configurations with two and four particles in the unique space is represented with a dashed line.

Hamiltonian responsible for this feature. Results when only the normal-parity spaces are included in the calculation (shown in parentheses) reveal a contribution of the unique-parity sector of only up to 2-3%. An increase in this number is expected for higher-lying states or heavier nuclei where the dominant configurations are the ones with an occupied unique-parity space.

Finally, let us look at the content of the eigenfunctions for the states in the different bands. In the g.s. ($K = 0^+$) band of ^{64}Ge , one can clearly see the dominance of the leading and most deformed SU(3) irrep (8, 4) (Fig. 6(a)) which gradually declines throughout the band from about 80% for $J = 0_{g.s.}^+$ to less than 40% for $J = 8_1^+$. Since the spin-orbit interaction is not as strong as in the case of the ds-shell nuclei, the mixing of irreps is smaller compared to the corresponding normal-SU(3) results for ^{24}Mg and ^{28}Si [9]. On the other hand, as mentioned above, the $K = 2^+$ band follows a less regular pattern with some of the states being of highly mixed nature. The 0_2^+ state is found to be dominated (85%) by the $(\lambda, \mu), S = (9, 2), 1$ irrep. In the case of ^{68}Se , the leading irrep (12, 0) contributes from 75 to 85% (Fig. 6(b)). A slight change in the type of Hamiltonian used may help establish the transition from states of prolate shape dominated by the irrep (12, 0) in the g.s. band to ones where the (0, 12) irrep prevails. To achieve this effect we need to add a term proportional to the third order Casimir invariant C_3 of SU(3). It was demonstrated earlier [9] that this term is capable of adjusting the prolate-oblate band crossing by driving irreps with $\mu \gg \lambda$ lower in energy than those with $\lambda \gg \mu$. The same term can also be used to fix the position of the first excited 0^+ state not assigned yet experimentally but predicted by our G-matrix calculations to lie at 1.05 MeV.

Although the extended-SU(3) calculations are performed in a model space that involves the whole gds shell, the basis is still much smaller in size even compared with the one used for realistic calculations in the $pf_{5/2}g_{9/2}$ space. This drastic reduction translates into the use of only hundreds or at most a few thousand basis states

(Table V). For example, the size of the basis used in the extended-SU(3) calculations for ^{64}Ge represents only between 0.02% to 0.3% of that for unrestricted calculations in the $pf_{5/2}g_{9/2}$ model space. This means that a space spanned by a set of extended-SU(3) basis states may be computationally manageable beyond the limit accessible for the modern full-space shell-model calculations as is the case for the combination of the upper-fp and the gds shells.

While some refinements in the model certainly could be done (like trying different and more sophisticated types of Hamiltonians, using different strengths for identical-particle and pn-pairing interactions, etc.) and the role of the model-space truncation may be further explored, the results presented in this paper suffice to demonstrate that the SU(3) scheme in its extended formulation can be a valuable tool for studying nuclei of the upper-fp-shell region. Its benefits will show even more prominently in the more general and complicated case, namely, when the dominant configuration is no longer the one with an empty unique-parity space and in situations when two or more competing configurations are closer to one another in energy and as a consequence experience strong mixing.

V. CONCLUSIONS

In this paper we extended the usual pseudo-SU(3) shell model for upper-fp shell nuclei in two ways: firstly by integrating the $g_{9/2}$ level into the dynamics; and secondly by including the entire gds-shell organized via its SU(3) structure, which we dubbed the extended SU(3) shell model. While this work only deals with the simplest case in which one configuration (the one with no particles in the unique-parity space) dominates all others, it is still possible to appreciate the strength of this new approach. Specifically, the model offers a richer model space compared to the previous SU(3) schemes by taking particles from the unique-parity space explicitly into account. As a result, the current approach presents an opportunity for a better description of the collectivity properties of the systems considered by reducing the effective charge needed in the description of their B(E2) transition strengths. These results will be even more pronounced for heavier systems where the intruder space is expected to have higher occupancy. This approach also offers an opportunity to explore the role of the intruder levels in the dynamics of the system as in the current study they are treated on the same footing as the normal-

parity orbitals. It is important to underscore that these advantages are accomplished within a highly truncated and symmetry-adapted basis, which possibly allows one to reach into otherwise computationally challenging (if not inaccessible) domains.

The results for the nuclei ^{64}Ge and ^{68}Se , presented in this paper, demonstrate a close reproduction of various results obtained with a realistic interaction. Specifically, many of the states in the energy spectra and the B(E2) transition strengths are nicely reproduced. While the results are satisfactory for the states from the g.s. bands, there still seem to be some need for a more precise description of the nuclear characteristics related to the properties of the eigenfunctions. These could be addressed in the future by including some corrections with the use of more elaborated interactions. Nevertheless, the results certainly suggest that the extended SU(3) model can be a valuable tool in studying properties of nuclei of special interest from this region, such as those lying close to the proton drip line or/and actively participating in the processes of nucleosynthesis. They also point to an excellent opportunity to reveal the role the intruder levels play in the dynamics of the system in an exciting and completely new way, namely, considering their connection to their like-parity partners within the framework of a severely-truncated symmetry-adapted model space.

An extension of the SU(3) shell model for the rare-earth and actinide nuclei is also underway. It will be able to provide some valuable new information and a better understanding of the fragmentation and clusterization phenomena in the B(M1) transition strengths. Also, it will significantly reduce the values of the effective charges used in estimates of the B(E2) transition strengths. In addition, an expected new emerging structure of the states in the excited $K = 0^+$ bands could give an explanation for the enhanced B(E2) transition strengths to members of the g.s. band. Finally, the new model provides a powerful means of explanation for the abundance of low-lying $K = 0^+$ states found experimentally.

Acknowledgments

This work was supported by the US National Science Foundation, Grant Numbers 0140300 and 0500291, and the Southeastern Universities Research Association (SURA). We would like to thank Piet Van Isacker for providing us with the realistic interactions used.

APPENDIX A: MONOPOLE PAIRING AND PAIR-SCATTERING IN THE FRAMEWORK OF THE EXTENDED SU(3) SHELL MODEL

The expression for the identical-particle pairing within a shell (and the identical-particle pair-scattering between two shells) in terms of SU(3) irreducible operators is given in [30]:

$$S^{\sigma\tau\dagger}S^{\sigma\tau'} = \frac{1}{2} \sum_{(\lambda_1, \mu_1)(\lambda_2, \mu_2)} \sum_{l'} (-)^{l-l'} \sqrt{(2l+1)(2l'+1)} \langle (\eta, 0)l; (\eta, 0)l \| (\lambda_1, \mu_1)10 \rangle \langle (0, \eta')l'; (0, \eta')l' \| (\mu_2, \lambda_2)10 \rangle$$

$$\times \langle (\lambda_1, \mu_1)10; (\mu_2, \lambda_2)10 \| (\lambda, \mu)10 \rangle_\rho \left[\left[a_{(\eta, 0)\frac{1}{2}}^\dagger \times a_{(\eta, 0)\frac{1}{2}}^\dagger \right]^{(\lambda_1, \mu_1)S_1=0} \times \left[\tilde{a}_{(0, \eta')\frac{1}{2}} \times \tilde{a}_{(0, \eta')\frac{1}{2}} \right]^{(\mu_2, \lambda_2)S_2=0} \right]_{\substack{\rho(\lambda, \mu), S=0; J=0 \\ \kappa=1L=0 \quad M_J=0}} \quad (\text{A1})$$

where $\sigma = \pi$ or ν with $\eta = \eta'$ ($\eta \neq \eta'$) and $\tau = \tau'$ ($\tau \neq \tau'$) for the case of pairing (pair-scattering). Here, $\langle ; \| \rangle$ denotes a reduced SU(3) \supset SO(3) Clebsch-Gordan coefficient and \tilde{a} is a proper SU(3) tensor defined by $\tilde{a}_{(0, \eta)l_j m} = (-)^{\eta+j+m} a_{(\eta, 0)l_j -m}$.

Using the fact that the $9-\lambda\mu$ ($9j$) coefficients connect composite tensors corresponding to different coupling schemes of four SU(3) (SU(2)) tensors, one can derive the corresponding expressions for the pn-pairing (pair-scattering) operators. The final result is given by

$$S^{\pi\nu, \tau\dagger}S^{\pi\nu, \tau'} = \frac{1}{4} \sum_{(\lambda_\pi, \mu_\pi)(\lambda_\nu, \mu_\nu)} \sum_{\mathcal{L}\mathcal{L}'\kappa_\pi\kappa_\nu} (-)^{l-l'} \sqrt{2\mathcal{L}+1} \sum_S \sqrt{2\mathcal{S}+1} \langle (\eta, 0)l; (0, \eta')l' \| (\lambda_\pi, \mu_\pi)\kappa_\pi \mathcal{L} \rangle$$

$$\times \langle (\eta, 0)l; (0, \eta')l' \| (\lambda_\nu, \mu_\nu)\kappa_\nu \mathcal{L}' \rangle \langle (\lambda_\pi, \mu_\pi)\kappa_\pi \mathcal{L}; (\lambda_\nu, \mu_\nu)\kappa_\nu \mathcal{L}' \| (\lambda, \mu)10 \rangle_{\rho'}$$

$$\times \left[\left[a_{(\eta, 0)\frac{1}{2}}^\dagger \times \tilde{a}_{(0, \eta')\frac{1}{2}} \right]^{(\lambda_\pi, \mu_\pi)\mathcal{S}} \times \left[b_{(\eta, 0)\frac{1}{2}}^\dagger \times \tilde{b}_{(0, \eta')\frac{1}{2}} \right]^{(\lambda_\nu, \mu_\nu)\mathcal{S}'} \right]_{\substack{\rho(\lambda, \mu), S=0; J=0 \\ \kappa=1L=0 \quad M_J=0}} \quad (\text{A2})$$

where $a^\dagger(a)$ and $b^\dagger(b)$ denote proton and neutron creation (annihilation) operators. Again, $\eta = \eta'$ ($\eta \neq \eta'$) and $\tau = \tau'$ ($\tau \neq \tau'$) for pn-pairing (pn-pair scattering). The labels (λ_π, μ_π) and (λ_ν, μ_ν) represent the proton and the neutron SU(3)-coupled irreps and the symbols \mathcal{L} and \mathcal{S} stand for the orbital and spin angular momentum in the coupled proton (and neutron) spaces.

-
- [1] M. G. Meyer, Phys. Rev. **75**, 1969 (1949); **78**, 16 (1950); **78**, 22 (1950); O. Haxel, J. H. D. Jensen, and H. E. Suess, *ibid.* **75**, 1766 (1949).
- [2] S. E. Koonin, D. J. Dean, and K. Langanke, Phys. Repts. **577**, 1 (1996).
- [3] J. P. Elliott, Proc. Roy. Soc. London, Ser. **A 245**, 128 (1958); **A 245**, 562 (1958).
- [4] R. D. Ratna Raju, J. P. Draayer, and K. T. Hecht, Nucl. Phys. **A202**, 433 (1973).
- [5] J. Escher, J. P. Draayer, and A. Faessler, Nucl. Phys. **A586**, 73 (1995).
- [6] K. H. Bhatt, C. W. Nestor, Jr., and S. Raman, Phys. Rev. C **46**, 164 (1992).
- [7] K. H. Bhatt, S. Kahane, and S. Raman, Phys. Rev. C **61**, 034317 (2000).
- [8] S. Åberg, H. Flocard, and W. Nazarewicz, Annu. Rev. Nucl. Part. Sci. **40**, 469 (1990).
- [9] C. Vargas, J. G. Hirsch, and J. P. Draayer, Nucl. Phys. **A690**, 409 (2001).
- [10] C. E. Vargas, J. G. Hirsch, and J. P. Draayer, Nucl. Phys. **A697**, 655 (2002).
- [11] G. Popa, J. G. Hirsch, and J. P. Draayer, Phys. Rev. C **62**, 064313 (2000); C. Vargas, J. G. Hirsch, T. Beuschel, and J. P. Draayer, Phys. Rev. C **61**, 031301(R) (2000).
- [12] H. Schatz et al., Phys. Rep. **294**, 167 (1998); J. A. Clark et al., Phys. Rev. C **75**, 032801(R) (2007).
- [13] K. Kaneko, M. Hasegawa, and T. Mizusaki, Phys. Rev. C **70**, 051301(R) (2004).
- [14] Y. Sun, M. Wiescher, A. Aprahamian, J. Fisker, Nucl. Phys. **A758**, 765c (2005).
- [15] E. Caurier, F. Nowacki, A. Poves, and J. Retamosa, Phys. Rev. Lett. **77**, 1954 (1996).
- [16] A. Abzouzi, E. Caurier, and A. P. Zuker, Phys. Rev. Lett. **66**, 1134 (1991). F. Nowacki, Ph. D. thesis, ULP Strasbourg, 1995 (unpublished).
- [17] S. M. Vincent et al., Phys. Lett. B **437**, 264 (1998).
- [18] P. Van Isacker, O. Juillet, and F. Nowacki, Phys. Rev. Lett. **82**, 2060 (1999).
- [19] K. P. Drumev et al., to be submitted to Nucl. Phys. A.
- [20] R.R. Whitehead and A. Watt, J. Phys. G **4**, 835 (1978);

- R.R. Whitehead et al., in *Theory and Application of moment methods in Many-Fermion systems*, edited by B. J. Dalton et al. (Plenum, New York, 1980); E. Caurier, A. Poves, and A. P. Zuker, *Phys. Lett.* **B252**, 13 (1990); *Phys. Rev. Lett.* **74**, 1517 (1995).
- [21] A. P. Zuker, J. Retamosa, A. Poves, and E. Caurier, *Phys. Rev. C* **52**, R1741 (1995); G. Martinez-Pinedo, A. P. Zuker, A. Poves, and E. Caurier, *Phys. Rev. C* **55**, 187 (1997); C. Vargas, J. G. Hirsch, P. O. Hess, and J. P. Draayer, *Phys. Rev. C* **58**, 1488 (1998).
- [22] P. Ring and P. Schuck, *The Nuclear Many-Body Problem* (Springer, Berlin 1979).
- [23] K. Kaneko, M. Hasegawa, and T. Mizusaki, *Phys. Rev. C* **66**, 051306(R) (2002).
- [24] M. Dufour, A. P. Zuker, *Phys. Rev. C* **54**, 1641 (1996).
- [25] National Nuclear Data Center, <http://www.nndc.bnl.gov>.
- [26] K. C. Tripathy and R. Sahu, *Int. Journ. Mod. Phys. E* **11**, 531 (2002).
- [27] S. M. Fischer, D. P. Balamuth, P. A. Hausladen, C. J. Lister, M. P. Carpenter, D. Seweryniak, and J. Schwartz, *Phys. Rev. Lett.* **84**, 4064 (2000).
- [28] J. P. Draayer and K. J. Weeks, *Ann. Phys. (N.Y.)* **156**, 41 (1984); O. Castaños, J. P. Draayer, and Y. Leschber, *ibid.* **180**, 290 (1987).
- [29] K. Starosta et al., *Phys. Rev. Lett.* **99**, 042503 (2007).
- [30] C. Bahri, J. Escher, and J. P. Draayer, *Nucl. Phys.* **A592**, 171 (1995).